Biomedicine & Pharmacotherapy 164 (2023) 114926

Contents lists available at ScienceDirect

Biomedicine & Pharmacotherapy

journal homepage: www.elsevier.com/locate/biopha

Pathologic HDAC1/c-Myc signaling axis is responsible for angiotensinogen transcription and hypertension induced by high-fat diet

Eui Kyung Youn [a], Hyun Min Cho [a], Jin Ki Jung [a], Ga-Eun Yoon [a], Masumi Eto [b], Jee In Kim [a,*]

[a] Department of Molecular Medicine, Keimyung University School of Medicine, Daegu 42601, Republic of Korea
[b] Department of Veterinary Medicine, Okayama University of Science, Ehime 794–8555, Japan

ARTICLE INFO

Keywords:
Obesity-associated hypertension
Histone deacetylase 1
Cellular myelocytomatosis oncogene
Angiotensinogen
Epigenetic regulation

ABSTRACT

High-fat diet (HFD)-induced obesity is a cause of resistant hypertension. We have shown a possible link between histone deacetylases (HDACs) and renal angiotensinogen (Agt) upregulation in the HFD-induced hypertension, whereas the underlying mechanisms remain to be elucidated. Here, using a HDAC1/2 inhibitor romidepsin (FK228) and siRNAs, we determined roles of HDAC1 and HDAC2 in HFD-induced hypertension and found the pathologic signaling axis between HDAC1 and Agt transcription. Treatment with FK228 canceled the increased blood pressure of male C57BL/6 mice induced by HFD. FK228 also blocked upregulation of renal Agt mRNA, protein, angiotensin II (Ang II) or serum Ang II. Activation and nuclear accumulation of both HDAC1 and HDAC2 occurred in the HFD group. The HFD-induced HDAC activation was associated with an increase in deacetylated c-Myc transcription factor. Silencing of HDAC1, HDAC2 or c-Myc in HRPTEpi cells decreased Agt expression. However, only HDAC1 knockdown, but not HDAC2, increased c-Myc acetylation, suggesting selective roles in two enzymes. Chromatin immunoprecipitation assay revealed that HFD induced the binding of HDAC1 and deacetylated c-Myc at the *Agt* gene promoter. A putative c-Myc binding sequence in the promotor region was necessary for Agt transcription. Inhibition of c-Myc downregulated Agt and Ang II levels in kidney and serum, ameliorating HFD-induced hypertension. Thus, the abnormal HDAC1/2 in the kidney may be responsible for the upregulation of the *Agt* gene expression and hypertension. The results expose the pathologic HDAC1/c-myc signaling axis in kidney as a promising therapeutic target for obesity-associated resistant hypertension.

1. Introduction

The rapid growth of obesity worldwide has led to the establishment of obesity-associated hypertension as a major cause of various complications and premature death [1]. Moreover, obesity is a cause of resistant hypertension, which constitutes 10–15% of hypertension cases. Individuals suffering obesity-associated hypertension are less likely to respond to appropriate blood pressure (BP) control measures despite the use of at least three antihypertensive drugs including inhibitors for angiotensin II (Ang II) [2]. Therefore, limitations exist in conventional AngII therapies for resistant hypertension, even though renin–angiotensin–aldosterone system activation represents a leading cause of the hypertension [3].

Epigenetics provides a new approach for diagnosis and prognosis of hypertension, and a new area of drug-discovery targets [4]. Our group previously reported that the broad spectrum histone deacetylase (HDAC) inhibitors, valproate and CG200745, inhibit high-fat diet (HFD)-induced expression of renal angiotensinogen (Agt), a precursor of Ang II, ameliorating obesity-associated hypertension in mice [5,6]. Clearly, HDACs are involved in Agt expression and HFD-induced hypertension. However, questions remain: Which classes of HDAC are responsible for the signaling? What are targets of HDACs? Can HDAC signaling be a therapeutic target for obesity-associated hypertension?

Lines of evidence suggest that the transcription factor cellular

Abbreviations: Agt, angiotensinogen; Ang II, angiotensin II; ChIP, chromatin immunoprecipitation; D1R, dopamine-1-receptor; HDAC, histone deacetylase; HEK-293, human embryonic kidney cell line; HFD, high-fat diet; HRPTEpi, human renal proximal tubule epithelial cell line; i.p., intraperitoneal (injection); ND, normal diet; PBS, phosphate-buffered saline; qRT-PCR, quantitative reverse transcription polymerase chain reaction; RT, room temperature; SDS-PAGE, sodium dodecyl sulfate-polyacrylamide electrophoresis; siRNA, small interfering RNA; S/P, streptomycin/penicillin.

* Correspondence to: Department of Molecular Medicine, Keimyung University School of Medicine 1095 Dalgubeol-daero, Dalseo-gu Daegu 42601, Republic of Korea.
E-mail address: jeein.kim@kmu.ac.kr (J.I. Kim).

https://doi.org/10.1016/j.biopha.2023.114926
Received 20 March 2023; Received in revised form 3 May 2023; Accepted 22 May 2023
Available online 26 May 2023

myelocytomatosis oncogene (c-Myc), a well-known proto-oncogene, is associated with hypertension. In spontaneously hypertensive rats (SHR), Ang II-dependent c-Myc activation facilitates vascular smooth muscle cell proliferation and hypertension. Conversely, an angiotensin converting enzyme inhibitor normalizes this proliferation by inhibiting c-Myc expression and its effects on the cell cycle [7]. c-Myc also raises BP in an Ang II-dependent manner by upregulating renal G protein-coupled receptor kinase 4, which negatively regulates dopamine-1-receptor (D1R). Inhibition of c-Myc activity restores coupling of D1R to adenylyl cyclase stimulation [8–10]. In addition, HFD fuels prostate cancer progression by amplifying the c-Myc signal [11]. Because HDAC inhibitor treatment downregulates c-Myc to promote cancer cell apoptosis in an acute myeloid leukemia model [12], we postulated that a novel signaling axis between HDACs and c-Myc plays a role in HFD-induced hypertension.

FK228 selectively inhibits HDAC1 and HDAC2, compared with other HDAC family members [13]. FK228 was approved by the United States Food and Drug Administration for the treatment of cutaneous T-cell lymphoma and peripheral T-cell lymphoma [14,15]. FK228 showed strong antitumor effect against tumor xenografts in mice concomitant with the suppression of c-Myc and induction of p21 [16]. However, potential of FK228 at any doses for the treatment of obesity-associated hypertension has yet to be tested. Herein, we examined possibility of anti-hypertensive effects of FK228 using an HFD-fed mouse model and investigated the mechanisms by which FK228 normalizes c-Myc to mediate HFD-induced Agt transcription and the associated hypertension.

2. Materials and methods

2.1. Animal experiments

All the animal experiments were conducted according to the guidelines of the National Institutes of Health for the Care and Use of Laboratory Animals. The experimental protocols (KM-2017–34R1 and KM-2019–28R1) were approved by the Institutional Animal Care and Use Committee at Keimyung University School of Medicine and the study complied with all ethical regulations. Male C57BL/6 mice (8 weeks old; Koatech, Inc., Gyeonggi-do, Korea) were used in this study. The mice were randomly assigned to receive either a control, normal diet (ND) or HFD, containing 10% or 60% kCal from fat, respectively (#TD.94048 and #TD.06414, Harlan Laboratories, Inc., Madison, WI, USA). After 12 weeks, the HFD-fed mice reached a hypertensive phase of over 140 mmHg systolic BP. The mice were divided into four groups: ND-fed mice treated with vehicle (Veh), ND-fed mice treated with FK228 (#ab143287, Abcam, Cambridge, UK) or 10058-F4 (#S7153, Selleckchem, Houston, TX, USA), HFD-fed mice treated with Veh, and HFD-fed mice treated with FK228 or 10058-F4. They were administered FK228 (#ab143287, Abcam, Cambridge, UK) at the dose of 100 μg/kg body weight (BW) per day or the vehicle (control) via intraperitoneal injection (i.p.) for 17 days. 10058-F4 was given at the dose of 20 mg/kg BW per day via i.p. for 15 days. The mice were kept on either ND or HFD during the treatment. Mice were anesthetized with pentobarbital sodium (50 mg/kg BW, i.p.). Organs were removed, immediately frozen in liquid nitrogen, and stored at − 80 °C until analysis.

2.2. BW measurement

BW of the mice fed ND or HFD was measured using a scale (#KC-300, AND KOREA, Seoul, Korea). During periods of administration of the vehicle or FK228, BWs were measured daily.

2.3. BP measurement

BP was measured using a noninvasive tail-cuff system (#CODA-HT4, CODA, Kent Scientific Corporation, Torrington, CT, USA) according to the manufacturer's instructions. Briefly, each mouse was pre-warmed on a hot plate at 35 °C for 10 min and then placed in a restrainer. A cuff with a pneumatic pulse sensor was attached to the tail and the mouse was placed on a 35 °C heating pad. BP values were recorded using a CODA High-Throughput Non-invasive Blood pressure system. The values from 10 consecutive readings were averaged per mouse [17].

2.4. Ang ll enzyme immunoassay

Ang II concentrations in the serum, liver, and kidney were measured using an Ang II enzyme immunoassay kit #EK-002–12 (Phoenix Pharmaceuticals, Inc., Mannheim, Germany) for serum or #MBS701638 (MyBioSource, Inc., San Diego, CA, USA) for tissues following the manufacturer's instructions. The Ang II concentrations of tissue homogenates or serum were determined using SigmaPlot (Systat Software, Inc., San Jose, CA, USA) based on a standard curve for Ang II generated using serial dilutions of Ang II ranging from 0.45 to 30 pg/mL. The detailed information is provided in supplementary method.

2.5. Quantitative reverse transcription-polymerase chain reaction (qRT-PCR) analysis

The total RNA of tissues or human renal proximal tubule epithelial (HRPTEpi) cell or HEK-293 (human embryonic kidney) cell lysates was extracted using PureHelix™ RNA extraction solution (#RES200, Nanohelix, Seoul, Korea). Subsequently, 1 μg of RNA was used for cDNA synthesis by using the DiaStar™ RT Kit (#DR23-R10k, SolGent Co., Daejeon, Korea). qRT-PCR was performed using LightCyclerR 480 SYBR Green I Master mix (#04707516001, Roche, Mannheim, Germany) and the LightCyclerR 96 real-time PCR system (#05815916001, Roche). Primer sequences were as follows (sense/antisense): 5′-CTCGAACTCAAAGCAGGAGAG-3′ and 5′-GTAGATGGCGAACAGGAAGG-3′ for mouse Agt; 5′-GTAACCCGTTGAACCCCATT-3′ and 5′-CCATCCAATCGGTAGTAGCG-3′ for mouse 18S ribosomal RNA; 5′-GGGATTGATGACGAGTCCTATG-3′ and 5′-GAGTCTGAGCCACACTGTAAG-3′ for human HDAC1; 5′-CCAGTG-TTTGATGGACTCTTTG-3′ and 5′-CAGCCCAATTA-ACAGCCATATC-3′ for human HDAC2; 5′-GAGACATGGTGAACCAGAGTT-3′ and 5′-CAGGTACAAGCTGGAGGTG-3′ for human c-MYC; 5′-AGTGGACGTAGGTGTTGAAAG-3′ and 5′-GATGTTGCTGCTGAGA-AGATTG-3′ for human Agt; 5′-CACTCTTCCAGC-CTTCCTTC-3′ and 5′-GTACAGGTCTTTGCGGATGT-3′ for human β-actin; 5′-GAACGAATCCCGCTCAAGAA-3′ and 5′-AGGAAGGCCTCTTTGTGAATAC-3′ for mouse renin; and 5′-GTACCTTTGGTCTCCCGACA-3′ and 5′-TGTCAGCCTCTTCATGGGTT-3′ for human renin.

2.6. Western blot analysis

Sodium dodecyl sulfate-polyacrylamide gel electrophoresis (SDS-PAGE) samples were prepared by lysing the liver, kidney, and HRPTEpi cell with a lysis buffer [5 mmol/L hydroxyethyl piperazine ethane sulfonicacid (pH 7.4), 5 mmol/L egtazic acid, 1 mmol/L Na_3VO_4, 1% Triton X-100, 10% glycerol, 1 mmol/L dithiothreitol, 5 mmol/L NaF, 1 mmol/L phenylmethylsulfonyl fluoride, 5 μg/mL leupeptin, 2 μg/mL aprotinin, and 1% sodium deoxycholate]. The samples were electrophoresed and transferred onto polyvinylidene fluoride or nitrocellulose membranes, and then subjected to immunoblotting with antibodies. Immunereactive bands were visualized using a chemiluminescence reagent (#32106, Pierce, Thermo Fisher Scientific or #NEL104001EA, PerkinElmer Inc., Waltham, MA, USA). Signal intensities were quantified using the image analysis software ImageJ (ver. 1.52a, National Institutes of Health, Bethesda, MD, USA). Primary antibodies used included those against Agt (#orb10088, Biobyt, Cambridge, UK), β-Actin (#sc-47778, Santa Cruz Biotechnology, Inc.), c-Myc (#13–2500, Invitrogen, Carlsbad, CA, USA), HDAC1 (#sc-81598x, Santa Cruz Biotechnology, Inc., Dallas, TX, USA), HDAC2 (#sc-7899x, Santa Cruz Biotechnology, Inc.),

GAPDH (#NB600–502, Novus Biologicals, Littleton, CO, USA), Histone H1 (#sc-8616, Santa Cruz Biotechnology, Inc.), and acetyl-c-Myc (Lys323) (#ABE26, Merck Millipore, Darmstadt, Germany). Horseradish-peroxidase-conjugated secondary antibodies against rabbit (#A120–101P, Bethyl Laboratories Inc., Montgomery, TX, USA) or mouse immunoglobulin G (IgG) (#A90–116P, Bethyl Laboratories Inc.) or goat IgG (#A50–101P, Bethyl Laboratories Inc.) were used.

2.7. HDAC1 and HDAC2 activity assays

HDAC1 and HDAC2 activities in the liver and kidney were measured using HDAC1 (#K342, BioVision Inc., Milpitas, CA, USA) and HDAC2 (#K341, BioVision Inc.) activity assay kit, respectively, following the manufacturer's instructions. Briefly, protein aliquots (100 ng) from tissue lysates were incubated with normal rabbit IgG or antibodies against HDAC1 or HDAC2 and protein A/G beads overnight at 4 °C on a rotary mixer. The protein/antibody/bead complex mixture was mixed with HDAC assay buffer and HDAC substrate and incubated at 37 °C for 2 h. Next, 100 μL of the mixture was put in well of the black plate, and the fluorophore values (excitation 380 nm/emission 500 nm) measured using a microplate reader (Infinite M200 pro & F200 pro, TECAN Group Ltd., Männedorf, Switzerland). The standard curve was plotted using 7-amino-4-trifluoromethyl coumarin, and the relative fluorescence units (RFU) of samples calculated using the standard curve.

2.8. Immunofluorescence

Periodate-lysine-paraformaldehyde-fixed kidneys were washed thrice with phosphate buffered saline (PBS), embedded in paraffin, and sectioned (3 μm thickness) using a microtome. Deparaffinization and rehydration were performed. After permeabilization with 0.1% triton x-100/PBS for 5 min, retrieval with 10 mmol/L sodium citrate buffer (pH 6.0) for 10 min, and blocking with 3% bovine serum albumin/PBS (w/v) for 1 h, the sections were incubated with primary antibodies against HDAC1 (#sc-81598x, Santa Cruz Biotechnology, Inc.), HDAC2 (#sc-9959, Santa Cruz Biotechnology, Inc.), c-Myc (#13–2500, Invitrogen), or acetylated c-Myc (Ac-c-Myc) (MycK323ac) (#C15410346, Diagenode, Liège, Belgium) at 4 °C overnight. After washing with PBS, the sections were incubated with biotinylated anti mouse IgG or biotinylated anti rabbit IgG (Vector Laboratories, Inc., Burlingame, CA, USA) at room temperature (RT) for 30 min. Then, Cy3-streptavidin (#43–4315, Invitrogen) was applied at RT for 1 h. The sections were mounted with 4′,6-diamidino-2-phenylindole-containing mounting solution (#DUO82040, Sigma-Aldrich Co.). Images were acquired using a confocal microscope (Carl Zeiss Microscopy GmbH, Jena, Germany). The fluorescent images were further quantitatively analyzed by ZEN 3.4 (Carl Zeiss GmbH, Ostfildern, Germany).

2.9. Chromatin immunoprecipitation (ChIP) assay

Kidney lysate was subjected to ChIP assays using a ChIP assay kit (EZ-ChIP™, #17–371, Millipore Corp., Billerica, MA, USA) following the manufacturer's instruction. Briefly, the kidney was homogenized in 1% formaldehyde in PBS for 1 min using a glass homogenizer, followed by cross-linking at RT for 9 min and centrifugation. Then, the pellet was lysed in the lysis buffer and sonicated thrice for 30 s with 60 s intervals using an ultrasonic processor (Sonic Dismembrator Model 100, Fisher Scientific, Loughborough, Leicestershire, UK) with 30% output for shearing the DNA into approximately 500 bp fragments. After centrifugation, the sheared DNA in the supernatant was immunoprecipitated with normal mouse or rabbit IgG or antibodies against HDAC1 (#sc-81598x, Santa Cruz Biotechnology, Inc.), HDAC2 (#sc-7899x, Santa Cruz Biotechnology, Inc.), c-Myc (#13–2500, Invitrogen) or acetylated c-Myc (#C15410346, Diagenode) with protein A-agarose beads containing salmon sperm DNA at 4 °C for overnight with rotation. The bead/antibody/chromatin complex was washed, followed by elution of the antibody/chromatin complex. Cross-linking was reversed and DNAs were purified; 10% of each DNA was used as input DNA. To design PCR primers for the ChIP assay, we analyzed 1100 bp of the promoter of the mouse *Agt* gene using the web promoter scan service AliBaba2.1 (TRANSFAC ver. 3.5). We designed primers encompassing segmented regions covering − 280 to − 170 bp, which contains the c-Myc binding site at − 208 to − 217 bp. The primer sequences (sense/antisense) were 5′-GTCACAACCCACTCAATCCT-3′ and 5′-TCATCTGCCAGTAGGGCT-3′.

2.10. HEK-293 cell culture and promoter activity analysis

HEK-293 cell was purchased from KCLB (#21573, Seoul, Korea) and cultured in minimum essential medium (#LM007–09, WELGENE Inc. Deagu, Korea) containing 10% fetal bovine serum (#10099–141, Gibco, Waltham, MA, USA) and 100 U/mL streptomycin/penicillin (S/P) (#LS202–02, WELGENE Inc.) at 37 °C in a humidified atmosphere containing 5% CO_2. For the reporter gene assay, the *Agt* gene promoter constructs were prepared as in Fig. 6A. The mouse *Agt* gene promoter was amplified by PCR and cloned into the pGL3-Basic vector (#E1751, Promega Corp., Fitchburg, WI, USA). Primer sequences used included (sense/antisense): 5′-TCAGATCCGGTACCGTTGCTC-TTCAGAGCCCATC-3′ and 5′-GGTGGCGAAGCTTTGA-GCCAAGCAGGCTTATTT-3′ for the *Agt* gene promoter region (pm) 1; 5′-TCAGATCCGCTAGCCAAAACCTCCAACCTCCAAA-3′ and 5′-GGTGGCGAAGCTTTGAG-CCAAGCAGGCTTATTT-3′ for *Agt* pm2; and 5′-TCAGATCCGCTAGCGAGGCTCATCTG-CCAGTAGG-3′ and 5′-GGTGGCGAAGCTTTGAGCCAAGCAGGCTTATTT-3′ for *Agt* pm3 (Fig. 6A). To determine whether c-Myc is important for Agt transcription, we substituted three nucleotides in the potential c-Myc binding site via site-directed mutagenesis using a kit (#E0552, New England BioLabs Inc., Ipswich, MA, USA) following manufacturer's instruction. Specifically, in the potential c-Myc binding site sequence (CCCAAGGCCA) in pm2, the third C was substituted with A for mutation (M)1, the fourth A with C for M2, and the sixth G with T for M3, or, all three nucleotides were substituted for M-all. The primer sequences (sense/antisense) were 5′-GGCCAGCCTATTTTTGCATGAGG-3′ and 5′-TTTGGTTACACATTTACCCCAGTTC-3′ for M1; 5′-GGCCAGCCTATTTTTGCATGAGG-3′ and 5′-TGGGGTTACACATTTACCCCAGTTC-3′ for M2; 5′-TGCCAGCCTATTTTTGCATGAGG-3′ and 5′-TTGGGTTACACATTTACCCCAG-TTC-3′ for M3; and 5′-TGCCAGCCTATTTTTGCATGAGG-3′ and 5′-TGTGGTTACAC-ATTTACCCCAGTTC-3′ for M-all. Successful substitution in the resulting construct was verified using DNA sequencing. The obtained plasmids were transfected into HEK-293 cells to measure promoter activities. HEK-293 cells at 50–60% confluence were incubated for 2 h in minimal essential medium containing 5% fetal bovine serum without S/P and then transfected with 500 ng vector (Agt pm1, pm2, pm3, M1, M2, M3, or M-all) using Lipofectamine 3000 for 48 h following the manufacturer's instruction. The promoter activities were measured using a luciferase assay system (#E1501, Promega Corp.) following the manufacturer's instruction. Briefly, we removed the growth medium from cultured cells, rinsed the cells in 1X PBS followed by lysis. Cell lysates were transferred to microcentrifuge tubes, briefly centrifuged, and the supernatant transferred to new tubes. Cell supernatant (20 μL) was mixed with 100 μL luciferase assay reagent and the luminescence was measured using a microplate reader (Infinite M200 pro & F200 pro, TECAN Group Ltd.).

2.11. Statistical analysis

The results are expressed as the means ± standard errors. Statistical significance was determined by Student's *t* test to analyze differences between 2 groups to compare the body weights and blood pressures. Differences between groups were considered statistically significant at a *p*-value of < 0.05. Statistical tests were performed using Microsoft Excel 2016.

3. Results

3.1. Inhibition of HDAC1 and HDAC2 by FK228 ameliorated HFD-induced hypertension

Eight-week-old male C57BL/6 mice were randomly divided into two groups and fed either an ND or HFD for 12 weeks and then treated with FK228 at 100 μg/kg BW per day by i.p, which is 10–50-times lower dose compared with anti-tumor treatment [18,19]. Prior to differential feeding, the average BW were not differed between two groups (22.00 ± 0.22 and 21.97 ± 0.19 g, ND vs. HFD). After 12 weeks, HFD group significantly increased BW compared to ND group (29.48 ± 0.42 and 44.38 ± 0.63 g; $p < 0.001$, ND vs. HFD at week 12) (Fig. 1A). In addition, the systolic BP significantly increased in in the HFD group (119 ± 2–148 ± 1 mmHg, $p < 0.001$, ND vs. HFD at week 12), but not in the ND group (119 ± 2–118 ± 1 mmHg) (Fig. 1B). Similarly, diastolic BP was significantly increased in the HFD group (92 ± 3–115 ± 1 mmHg, $p < 0.001$, ND vs. HFD at week 12), but not in the ND group (93 ± 2–91 ± 2 mmHg)

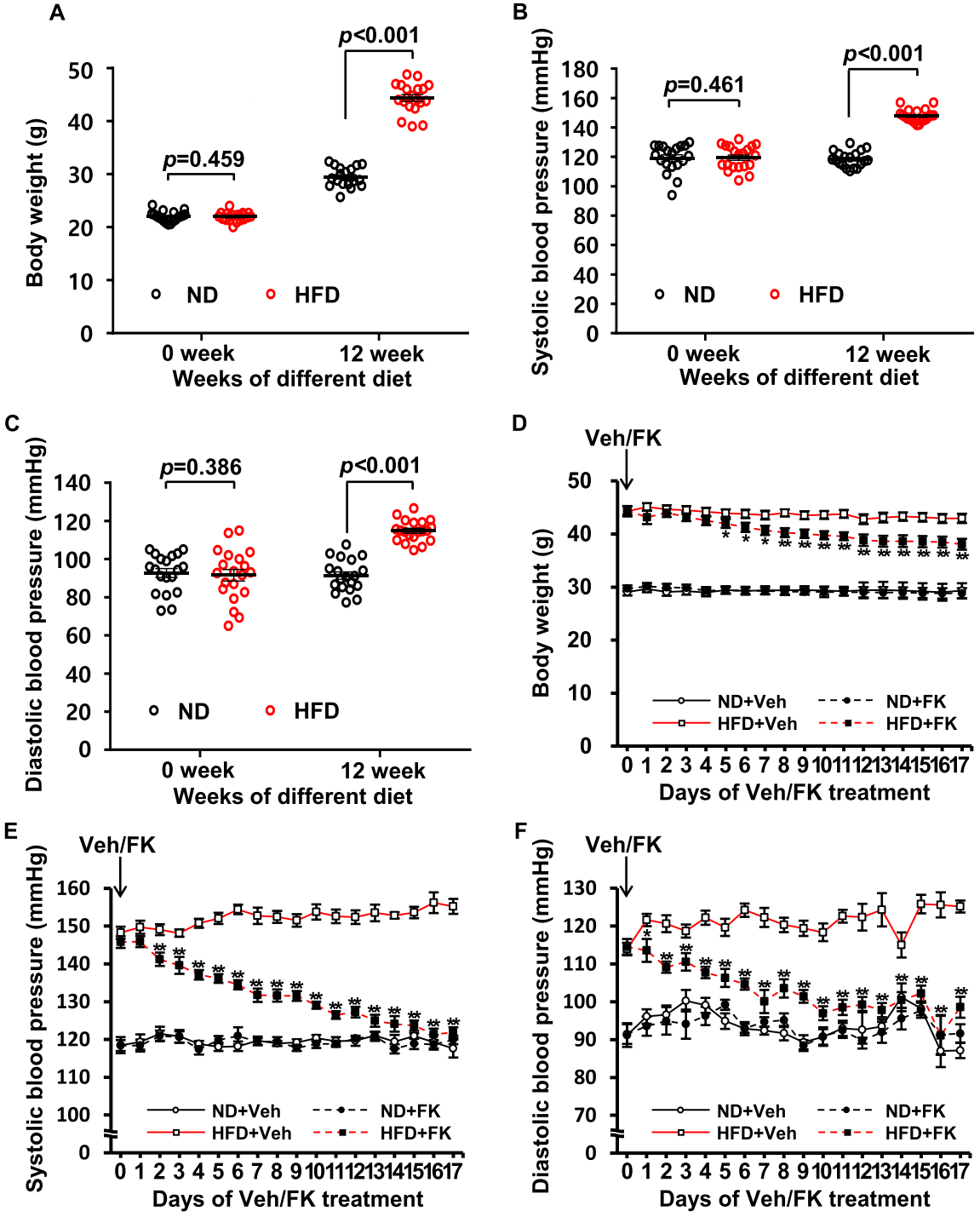

Fig. 1. Changes in BW and BP by HFD and the effect of FK228. BW (**A**), systolic BP (**B**), and diastolic BP (**C**) were measured before and after 12 w diet regimens. BW (**D**), Systolic BP (**E**), and diastolic BP (**F**) were measured during vehicle or FK228 (100 μg/kg BW per day) administration after the 12 w diet regimens. Results are expressed as the mean ± SE (n = 9–10 mice per group) (* $p < 0.05$ and ** $p < 0.01$ HFD+Veh vs. HFD+FK). Data were analyzed using the Student's t-test. BW, body weight; BP, blood pressure; SE, standard error; ND, normal diet; HFD, high-fat diet; Veh, vehicle; FK, FK228.

(Fig. 1C). As shown in Fig. 1D, BW was unchanged by the treatment with FK228 until 7 days, and then a subtle decrease in BW occurred in the HFD group (44.46 ± 0.82–38.08 ± 1.04 g) ($p < 0.01$, HFD Veh vs. HFD FK228 at day 17) (Fig. 1D). On the other hand, systolic BP (146 ± 2–122 ± 1 mmHg, $p < 0.01$, HFD Veh vs. HFD FK228 at day 17) (Fig. 1E) and diastolic BP (115 ± 2–99 ± 3 mmHg, $p < 0.01$, HFD Veh vs. HFD FK228 at day 17) in the HFD group were significantly decreased from day 2 of FK228 treatment and reached to the levels of the ND group by day 14 (Fig. 1E and F), suggesting FK228 administration can reverse HFD-induced hypertension with minimum effects on BW. It should be noted that FK228 treatment did not affect BW, systolic nor diastolic BP in the ND group, suggesting negligible adverse effects at this dose.

3.2. Renal Agt and Ang II were increased by HFD and reversed by FK228

To determine the underlying mechanisms of the anti-hypertensive activity of FK228, we determined effects of FK228 administration on Agt mRNA and protein level and Ang II concentration. Assay was conducted using kidney and serum, plus liver for evaluating tissue specificity. Kidney Agt mRNA and protein levels were both enhanced by HFD (2.39 ± 0.42 fold, p=0.004, ND Veh vs. HFD Veh) (Fig. 2A); (2.37 ± 0.24 fold, p=0.002, ND Veh vs. HFD Veh) (Fig. 2B), respectively. FK228 administration decreased the mRNA (p=0.004, HFD Veh vs. HFD FK228) (Fig. 2A) and protein ($p = 0.047$, HFD Veh vs. HFD FK228) (Fig. 2B) levels of Agt in kidney. Similarly, the level of Ang II in kidney was also enhanced by HFD (2.06 ± 0.13 pg/protein μg, p=0.003, ND Veh vs. HFD Veh) and decreased by FK228 ($p = 0.005$, HFD Veh vs. HFD FK228) (Fig. 2C). In parallel with the changes in kidney, serum Ang II concentration increased by HFD (4.97 ± 0.93 ng/mL, $p = 0.021$, ND Veh vs. HFD Veh). FK228 administration decreased serum Ang II in the HFD group ($p = 0.041$, HFD Veh vs. HFD FK228) (Fig. 2D). Liver Agt mRNA and protein levels were both enhanced by HFD (2.57 ± 0.33 fold, p=0.001, ND Veh vs. HFD Veh) (Fig. 2E); 2.07 ± 0.16 fold, $p < 0.001$, ND Veh vs. HFD Veh (Fig. 2F), respectively. Unlike kidney response, FK228 administration did not affect the mRNA (Fig. 2E) and protein (Fig. 2F) levels of Agt in liver. The level of Ang II in liver was not enhanced by HFD and decreased by FK228 (Fig. 2G). These data suggest that FK228 selectively suppresses transcription of Agt in the kidney of HFD group.

3.3. HFD increased the activities of HDAC1 and HDAC2, which were reversed by FK228 in mouse kidney

We next determined effects of FK228 administration on HDAC activities in the extracts of kidney and liver of the HFD group. HFD increased the activity of HDAC1 (2.43 ± 0.21 fold, p=0.001, ND Veh vs. HFD Veh) (Fig. 3A) and that of HDAC2 (1.76 ± 0.05 fold, $p < 0.001$, ND Veh vs. HFD Veh) (Fig. 3B), suggesting upregulation of active HDAC1/2. FK228 administration canceled the HFD-induced HDAC activation (p=0.002, HFD Veh vs. HFD FK228) (Fig. 3A) and HDAC2 ($p < 0.001$, HFD Veh vs. HFD FK228) (Fig. 3B) in kidney. By sharp contrast, HFD induced no significant changes in HDAC1/2 activities in liver (Fig. 3C and D). The basal HDAC activities were suppressed by FK228 administration (HDAC1; p=0.007, HFD Veh vs. HFD FK228 and HDAC2; p=0.033, HFD Veh vs. HFD FK228) (Fig. 3C, D). Thus, the upregulation of active HDAC1 and HDAC2 selectively occurs in the kidney of the HFD group, and it is normalized by FK228 administration.

3.4. HFD increased levels of nuclear HDAC1, HDAC2 and c-Myc, in parallel with deacetylation of c-Myc

We determined the expression levels of HDAC1, HDAC2 and c-Myc, and levels of acetylated c-Myc at K323 in the kidney of HFD group ± FK228 administration using fluorescent immunohistochemistry with antibodies for HDAC1, HDAC2, c-Myc, and Ac-c-Myc. In the section of the HFD group, nuclear staining of HDAC1 was prominent, compared with the ND group ($p < 0.001$, ND Veh vs. HFD Veh) and the FK228 treatment attenuated the accumulation ($p < 0.001$, HFD Veh vs. HFD FK228) (Fig. 4A and B). Similar staining pattern was observed in HDAC2 (Fig. 4A and C). Anti-c-Myc stain was diffused in the cytoplasm of the ND group and accumulated in the nuclei of the HFD group ($p < 0.001$, ND Veh vs. HFD Veh). FK228 significantly reduced the nuclear accumulation of c-Myc in the HFD group ($p < 0.001$, HFD Veh vs. HFD FK228) (Fig. 4A and D). Ac-c-Myc was found in the nuclei of the ND group, but the acetylation level was reduced in the HFD group ($p < 0.001$, ND Veh vs. HFD Veh). The Ac-c-Myc level was returned to the level of ND after the FK228 treatment ($p < 0.001$, HFD Veh vs. HFD FK228) (Fig. 4A and E).

3.5. Recruitment of c-Myc and HDAC1 to the Agt gene promoter was increased by HFD

As shown in Fig. 5A, a putative c-Myc binding site (−217 to −208 bp) was detected in the *Agt* gene promoter region (Fig. 5A). The chromatin complexes of the kidney of the HFD group were subjected to ChIP assay to determine whether HDAC1 or HDAC2 forms a complex with c-Myc, at the *Agt* gene promoter. The binding of c-Myc to the promoter region was increased in the HFD group, compared with ND (Fig. 5B). FK228 treatment eliminated the interaction of c-myc with the promoter (Fig. 5B). Notably, the binding of HDAC1 to the promoter was enhanced by HFD and was reversed upon FK228 administration (Fig. 5C). Conversely, antibodies targeting HDAC2 and Ac-c-Myc failed to capture the c-Myc binding site at the promoter (Fig. 5D and E). These results suggest that the binding of HDAC1 and c-Myc to the *Agt* gene promoter is necessary for the HFD-induced Agt upregulation.

3.6. Mutation of the c-Myc binding site decreased Agt gene promoter activity

To evaluate the importance of c-Myc binding for the Agt transcription, we conducted the reporter gene assay using constructs carrying various portions of the *Agt* gene promoter region and/or substitutions at the putative c-Myc binding sequence (Fig. 6A). As shown in Fig. 6B-C, the promoter activity of pm2 was significantly higher than those of pm1 and pm3. Thus, the region between − 625 and − 193 is necessary for the *Agt* promoter activity and the − 957 to − 625 bp region possibly functions as repressor (Fig. 6B). The substitutions of bases in the putative c-Myc binding site of pm2 (Fig. 6C) significantly decreased the promoter activity, suggesting that the c-Myc binding to the site is necessary for the Agt transcription (Fig. 6D).

3.7. Inhibition of c-Myc by 10058-F4 ameliorated HFD-induced renal Agt transcription and hypertension

Roles of c-Myc in HFD-induced Agt transcription and hypertension were determined using a c-Myc inhibitor 10058-F4. A 15-day administration of 10058-F4 (20 mg/kg BW per day, i.p.) did not affect BW in the ND and HFD group (Fig. 7A). After the 6-day-administration with 10058-F4, levels of BP were gradually and significantly declined in the HFD group [systolic BP: 149 ± 2–119 ± 2 mmHg ($p < 0.001$, HFD Veh vs. HFD 10058-F4 at day 15) diastolic BP: 115 ± 3–92 ± 1 mmHg ($p < 0.001$, HFD Veh vs. HFD 10058-F4 at day 15)] (Fig. 7B, C). Importantly, neither systolic nor diastolic BP level in the ND group was changed (Fig. 7B, C). The 10058-F4-induced decreases in BP levels of the HFD group occurred in parallel with decreases in the renal Agt mRNA level ($p < 0.001$, HFD Veh vs. HFD 10058-F4) (Fig. 7D), the renal AngII level ($p = 0.007$, HFD Veh vs. HFD 10058-F4) and the serum Ang II concentration ($p = 0.017$, HFD Veh vs. HFD 10058-F4). These data suggest that c-Myc inhibition using 10058-F4 mimics the action of HDAC1/2 inhibition by FK228.

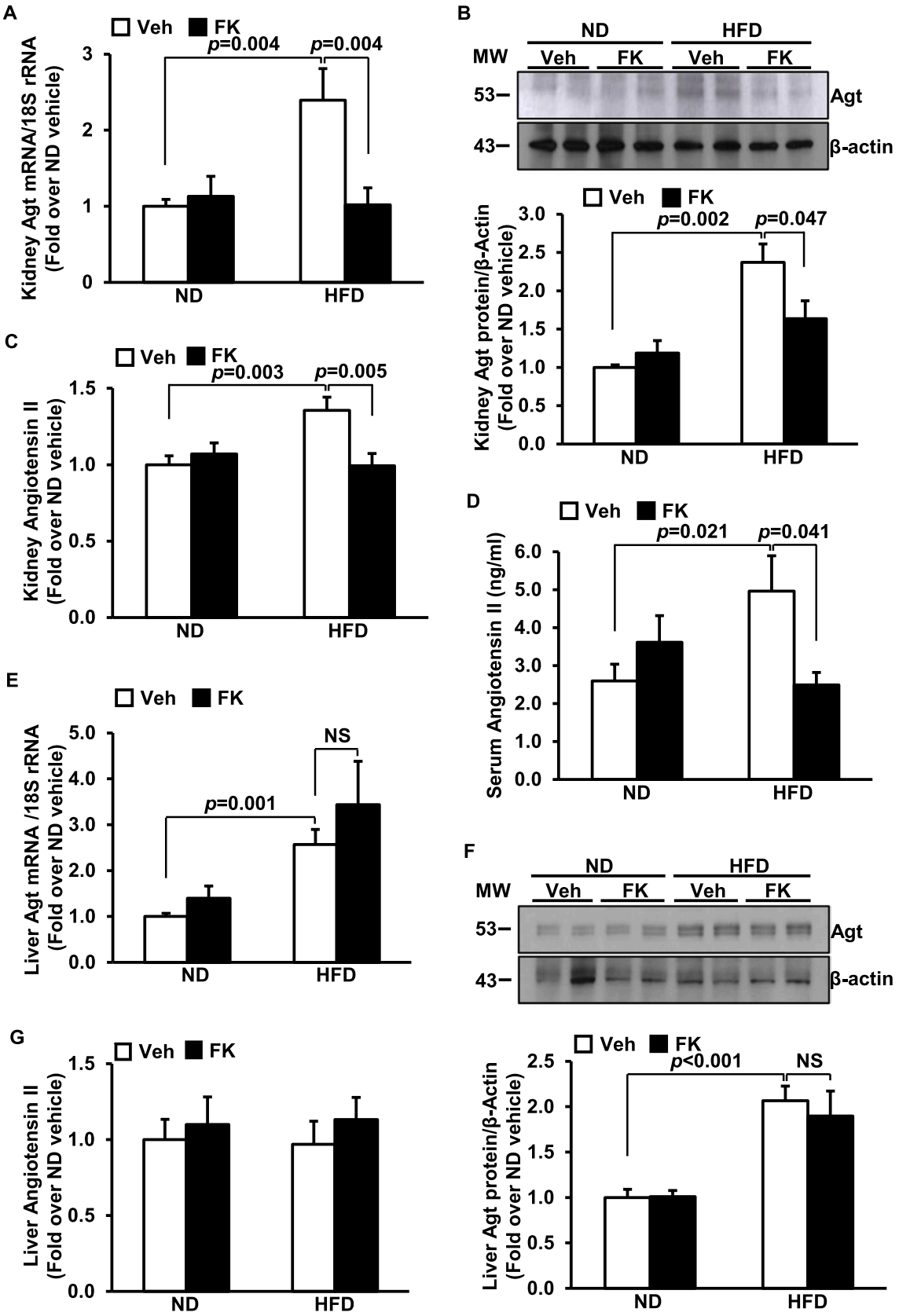

Fig. 2. Effects of HFD and FK228 on Ang II level and Agt mRNA and protein expression in mice. Graphs demonstrate the mRNA, protein with representative western blots, and Ang II in kidney (**A, B, C**) and liver (**E, F, G**) of ND- or HFD-fed mice after vehicle or FK228 administration. The serum Ang II levels were summarized in figure D. Results are expressed as the mean ± SE (n = 3–5 mice per group). Data were analyzed using the Student's t-test. ND, normal diet; HFD, high-fat diet; Veh, vehicle; FK, FK228; SE, standard error; MW, molecular weight (kDa); Ang II, angiotensin II; Agt, angiotensinogen; 18 S rRNA, 18 S ribosomal RNA; NS, no significance.

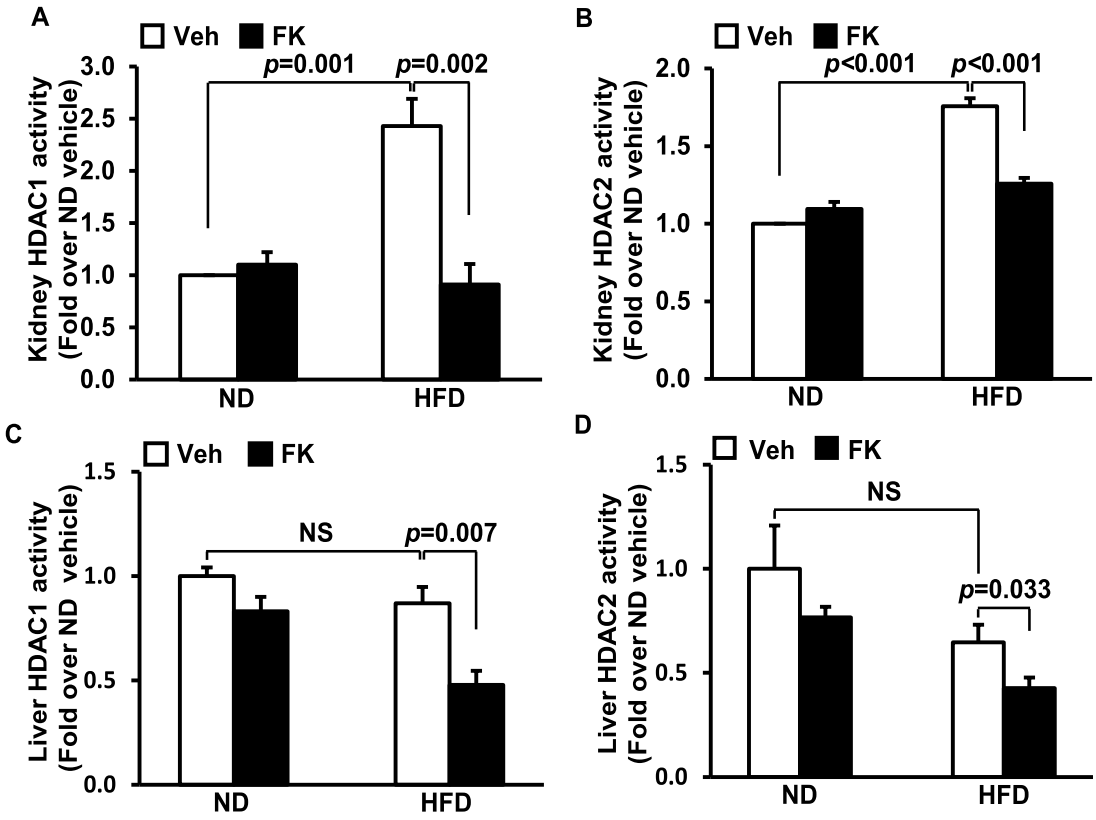

Fig. 3. Effects of HFD and FK228 on the activities of HDAC1 and HDAC2 in kidney and liver. Activities of HDAC1 and HDAC2 in the kidney (A and B) and liver (C and D) of ND- or HFD-fed mice after vehicle or FK228 administration. Results are expressed as the mean ± SE (n = 3–5 mice per group). Data were analyzed using the Student's t-test. ND, normal diet; HFD, high-fat diet; Veh, vehicle; FK, FK228; HDAC, histone deacetylase; SE, standard error; NS, no significance.

4. Discussion

The results of the present study demonstrate that HFD-induced hypertension can be attributed to the HDAC1/c-Myc axis activation and consequent renal Agt expression. A model is illustrated in Fig. 7G, in which HFD activates HDAC1 and triggers the HDAC1/c-Myc complex formation at the c-Myc binding site of the *Agt* gene promoter, resulting in the increased expression. HFD activates HDAC1, resulting in deacetylation of c-Myc and the binding of c-Myc to the promoter of *Agt* gene. The binding of c-Myc at the promoter elevates the Agt transcription and Ang II level in the kidney and serum. Because Agt upregulation in liver was insensitive to FK228 administration, we anticipate the HDAC1 action in kidney is responsible for the increased renal Ang II and hypertension. The selective HDAC1/2 inhibitor FK228 [20] inhibited HDAC1 activation, c-Myc deacetylation, HDAC1/c-Myc complex formation, binding of the HDAC1/c-Myc complex to the *Agt* gene promoter, renal and serum Ang II, and ultimately hypertension induced by HFD. Importantly, treatment with the c-Myc inhibitor also attenuated HFD-induced increase in Agt transcription and Ang II in the kidney and serum Ang II ameliorating hypertension. Thus, both HDAC1 and c-Myc seem to be good candidates for therapeutic intervention of obesity-induced hypertension.

Renin-angiotensin system activation is a key mechanism of obesity-associated hypertension [21]. Evidence strongly suggests that Agt is produced primarily by hepatic cells and secreted into the circulation to regulate angiotensin I and II levels in the plasma [22,23] and kidney [24]. Matsusaka et al. demonstrated a contribution of Agt production in the liver to renal Agt protein and Ang II levels using liver or kidney-specific Agt knockout (KO) mice, although the authors did not rule out the possibility that, under some conditions, renal Agt contributes to the renal Ang II synthesis to a significant extent [24]. In fact, kidney has been suggested to generate and regulate intrarenal Agt and Ang II [25] and elevations in both mRNA and protein Agt levels have been reported in the kidney of multiple hypertension models, such as Dahl salt-sensitive hypertensive rats, SHR, Ang II-dependent hypertensive rats, and various kidney diseases [26]. Under pathologic conditions, renal Agt system maybe involved in blood pressure dysregulation.

It should be also noted that, although using the knock-out mice Matsusaka et al. demonstrated that Agt protein produced in the proximal straight tubule is directly excreted into urine and not retained in the kidney [24], a growing body of evidence has shown that urinary Agt is a specific biomarker for the pathologic status of the intrarenal renin-angiotensin-aldosterone and hypertension [27]. Kobori et al. have shown that an increase in urinary Agt is associated with an augmentation of renal angiotensinogen expression and Ang II levels in the kidney [28,29]. In addition, overweight individuals have higher mRNA levels of urinary Agt, a reflection of intra-tubular renin–angiotensin (RAS) activation [30]. HFD-induced type2-diabetic mice also exhibit an augmentation of Agt excretion in urine without showing signs of albuminuria and renal fibrosis, suggesting that urinary Agt is an early and accurate indicator of intrarenal RAS activation and is important for renal Agt levels [31]. In the same context, Kukida et al. demonstrated that liver supplies the bulk of Agt protein to the kidney in humans and nonhuman primates, independent of the presence of renal Agt mRNA using antisense oligonucleotides targeting liver-drived human Agt (Gal-NAc Agt ASO) [32]. Therefore, although liver may supply Agt to the kidney under normal conditions, we cannot rule out the possibility that under some pathologic conditions, including obesity renal Agt may play roles in inducing hypertension.

In a rat model of chronic kidney disease with hypertension, the use of liver-targeted Agt siRNA led to a reduction of over 95% in plasma Agt levels, along with a significant decrease in Ang II expression in the

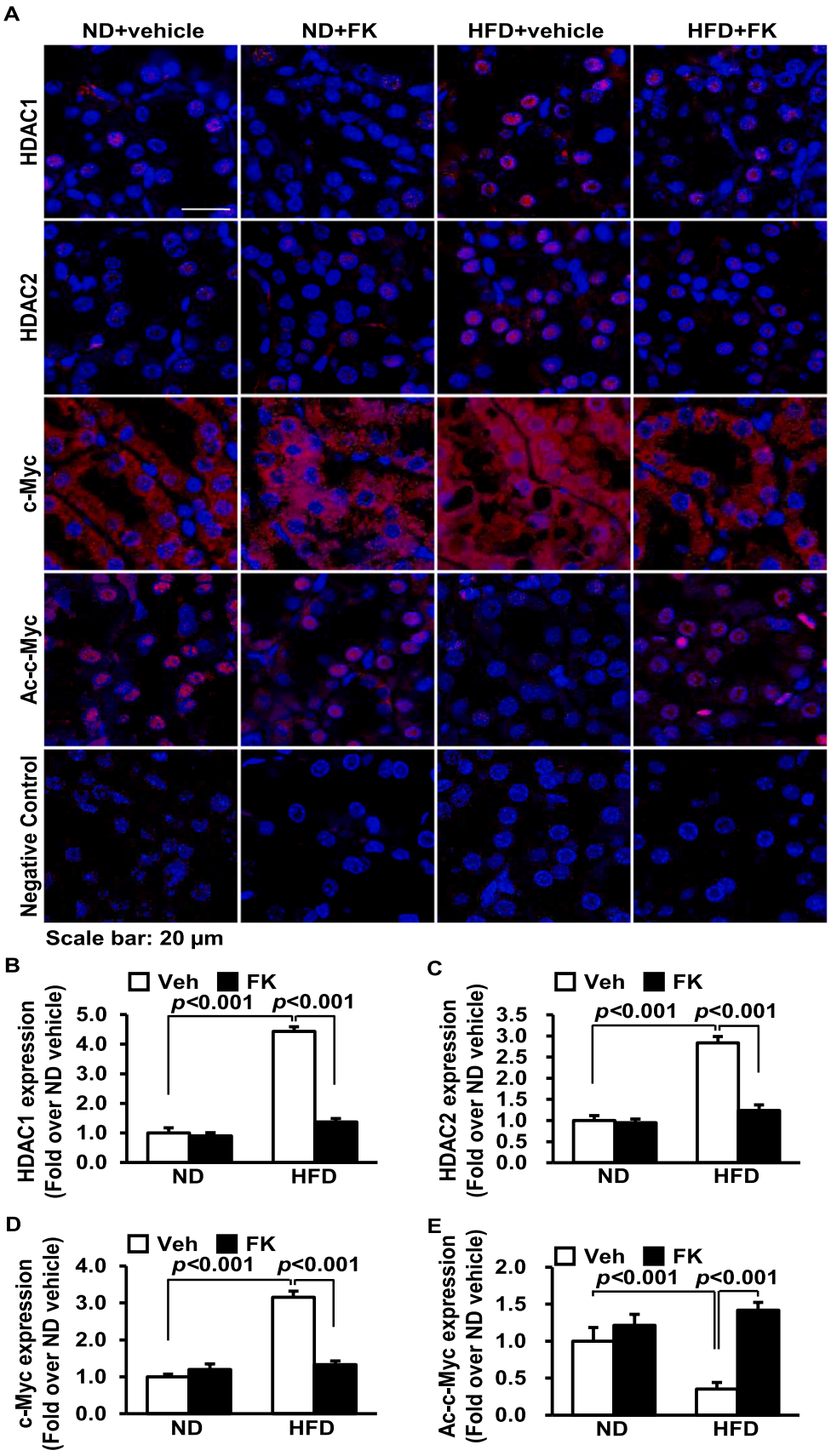

Fig. 4. Visualizations of HDAC1, HDAC2, c-Myc, and Ac-c-Myc with or without FK228 administration in ND- and HFD-fed mice kidney. (**A**) Immunofluorescence staining (red) shows HDAC1, HDAC2, c-Myc, and Ac-c-Myc with or without FK228 administration in ND or HFD-fed mice kidney. DAPI (blue), indicates nuclei. Staining with a secondary antibody only was used as a negative control for immunofluorescence staining. (**B-E**), Graphs summarize quantitative analysis of red fluorescence in kidney nuclei. Results are expressed as the mean ± SE. Data were analyzed using the Student's t-test. Original scale bar is 20 μm. ND, normal diet; HFD, high-fat diet; Veh, vehicle; FK, FK228; HDAC, histone deacetylase; c-Myc, cellular myelocytomatosis oncogene; Ac-c-Myc, acetylated c-Myc; DAPI, 4′,6-diamidino-2-phenylindole; SE, standard error.

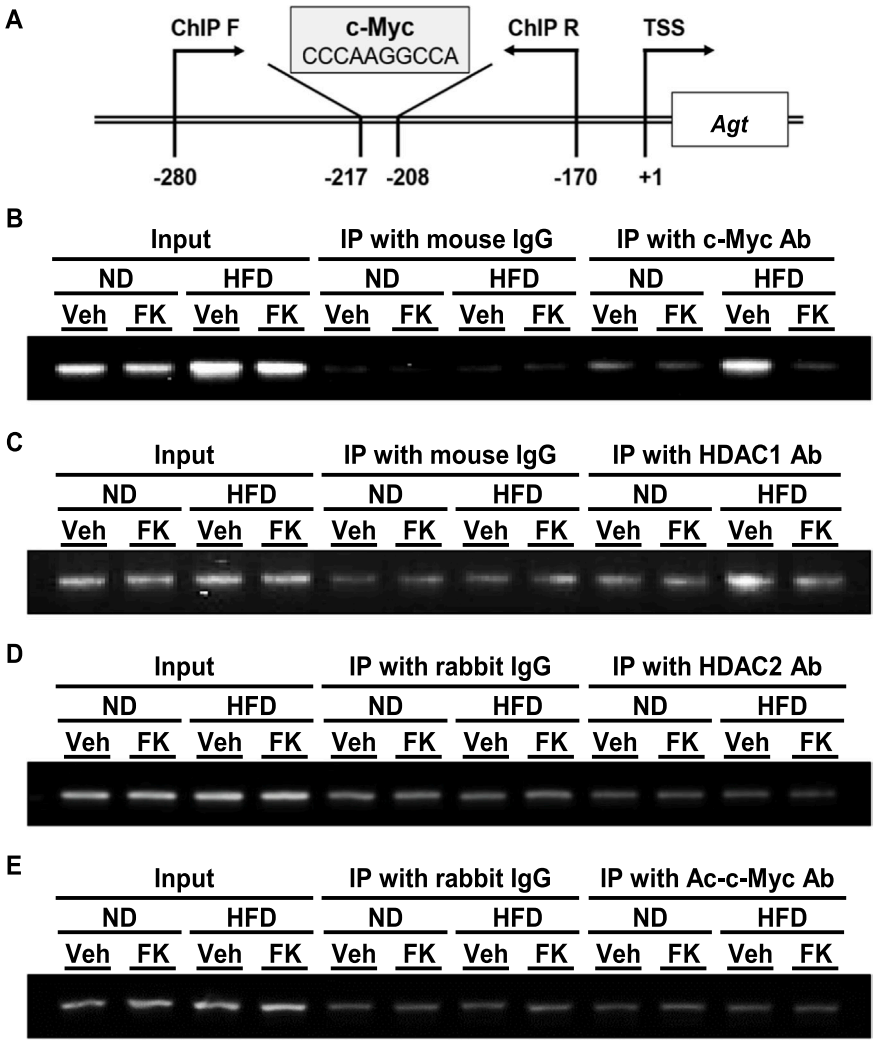

Fig. 5. Effect of FK228 on the HFD-induced binding of c-Myc and HDAC1 to the *Agt* gene promoter in mice kidney. (**A**) Schematic of ChIP PCR to show the PCR region and location of the putative c-Myc binding site in the *Agt* gene promoter. (B-E), Representative ChIP PCR results using corresponding antibodies. Binding of c-Myc (B), HDAC1 (C), HDAC2 (D), and Ac-c-Myc (E) to the putative c-Myc binding site in the *Agt* gene promoter in ND- or HFD-fed mice kidney following vehicle or FK228 administration. Normal mouse or rabbit IgG was used as a negative control for ChIP assays. ChIP, chromatin immunoprecipitation; PCR, polymerase chain reaction; ChIP F, forward primer for ChIP PCR; ChIP R, reverse primer for ChIP PCR; TSS, transcription starting site; Agt, angiotensinogen; c-Myc, cellular myelocytomatosis oncogene; HDAC, histone deacetylase; Ac-c-Myc, acetylated c-Myc; IP, immunoprecipitation; ND, normal diet; HFD, high-fat diet; Veh, vehicle; FK, FK228; IgG, immunoglobulin G; Ac-c-Myc, acetylated c-Myc; Ab, antibody.

kidney. However, Agt siRNA did not lower blood pressure [33]. In addition, the hepatocyte-directed antisense oligonucleotide drug, IONIS-AGT-LRx, designed to target Agt mRNA, resulted in a robust reduction of plasma Agt in subjects with hypertension along with only marginal reduction in blood pressure [34]. It is noteworthy that our finding show that the suppression of renal Agt levels with HDAC1 or c-myc inhibitors is capable of alleviating blood pressure levels, suggesting a new axis for the treatment.

Of note, the transgenic mice with Agt overexpression in proximal tubule caused the corresponding hypertension with or without liver Agt overexpression [35]. Koizumi et al. also demonstrated that Agt filtered through the glomerulus and reabsorbed via megalin by the proximal tubule is converted to Ang II resulting in sodium retention [36]. However, the data were obtained under extreme conditions, where a very severe nephrotic syndrome was rapidly developing. Translating the role of megalin in renal Ang II generation to all proteinuric conditions is therefore not yet possible [37]. In this paper, to rule out the effect of renin on renal Agt expression we determined renin levels in the FK or c-Myc inhibitor-treated HFD-fed mouse kidney and HDAC1 gene silenced HEK293 cells. Renin mRNA expression was increased by HFD and decreased by FK treatment but HDAC1 knock down did not affect renin mRNA level. Moreover, treatment of c-Myc inhibitor did not decrease renin mRNA level even though it lowered blood pressure with decreased renal Agt and Ang II (Supplementary Figure 5A, B, C). We postulate that the contribution of renin to HDAC1/c-Myc axis-induced renal Ang II increase induced by HFD is minimal.

Our group also has previously reported increased renal Agt transcription and the ameliorating effect of broad spectrum HDAC inhibitors in HFD-induced hypertension [5,6]. Here we showed that FK228 effectively lowered both systolic and diastolic BP in parallel with decreases in Agt and Ang II, plus the HDAC activity, in kidney but not in liver. Thus, at least in our HFD model, Agt upregulation in kidney seems to be the primary cause of the elevated BP levels. The c-Myc-dependent upregulation of Agt expression likely elevates local Ang II concentration in kidney driving the hypertensive phenotype. Our data do not eliminate roles of the *Agt* gene regulation in liver and other tissues in obesity-associated hypertension and the extent of the contributions should be addressed in further study. Nonetheless, it is noteworthy that our model in Fig. 7G interprets the action of FK228 and 10058-F4 lowering HFD-induced higher BP levels and supports the pathologic HDAC1/c-Myc axis as a new therapeutic target. Due to distinct tissue distribution and cellular localization of individual HDACs, selective HDAC inhibitors are considered to possess better therapeutic index and fewer adverse effects [38]. Further, the FK228 dose we used here corresponds to a 2–10% level of the dose the other researchers used and did not decrease BW of the control group [18,19]. Thus, our data expose a potential of HDAC1/2 inhibitors as a pharmacological antihypertensive regimen in renal Ang II-associated hypertension.

The enhanced transcription of Agt following HFD is attributed to enhanced binding of glucocorticoid receptor, CCAAT/enhancer-binding protein β, and signal transducer and activator of transcription 3 in hepatic and adipose tissues [39]. However, to the best of our knowledge,

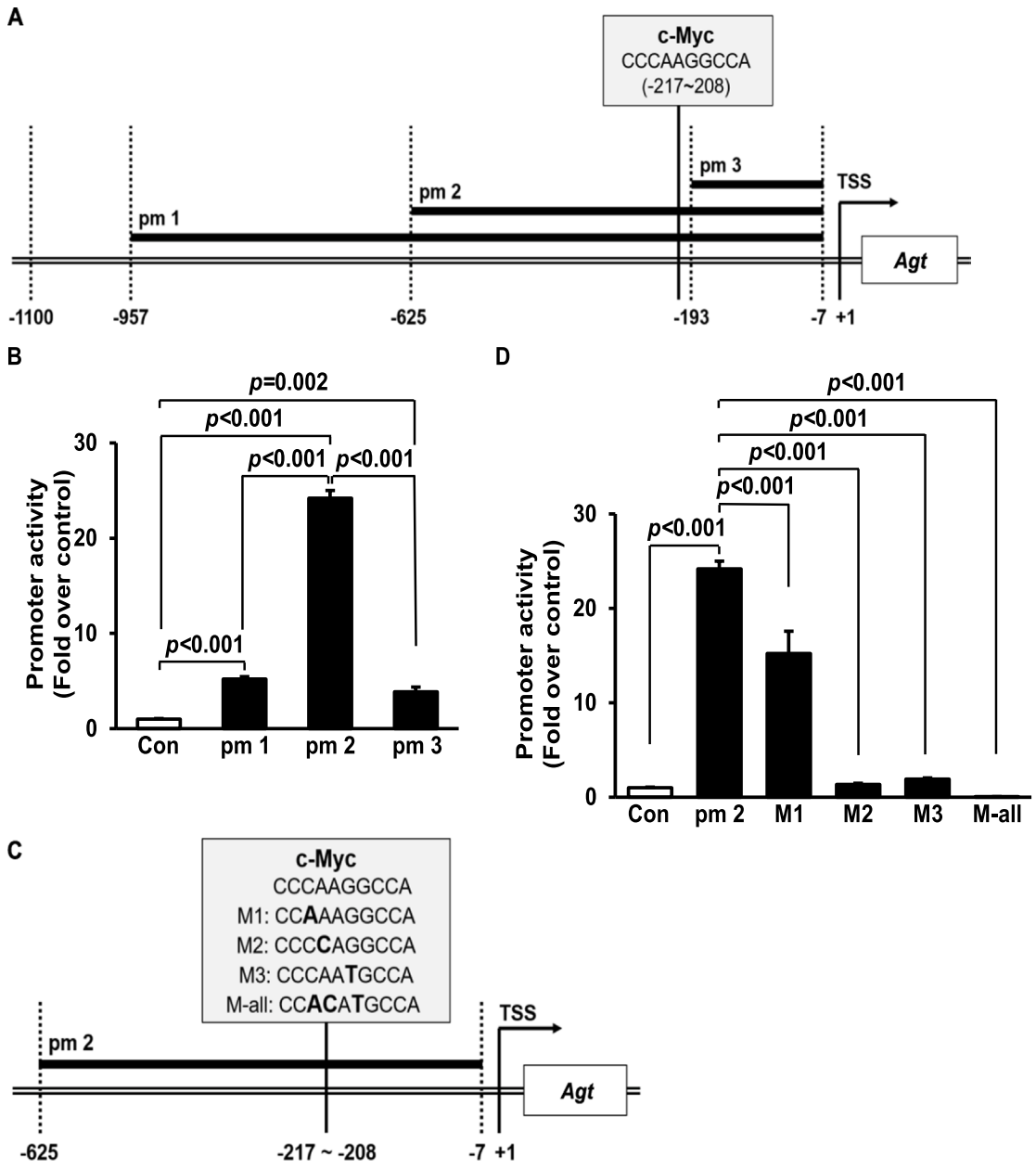

Fig. 6. Activities of *Agt* gene promoter fragments containing intact or mutated c-Myc binding sites. (A), Schematic of the DNA fragments used for promoter activity analysis and location of the putative c-Myc binding site in the *Agt* gene promoter. (**B**), Activities of the different regions in the *Agt* gene promoter. (**C**), Summary of the mutations in the c-Myc binding site in pm2 of the *Agt* gene promoter. (**D**), Activities of each mutant promoter. Results are expressed as the mean ± SE (n = 3 per group). Data were analyzed using the Student's t-test. pm, promoter; TSS, transcription starting site; Agt, angiotensinogen; c-Myc, cellular myelocytomatosis oncogene; SE, standard error; Con, control; M, mutation.

the transcription factors that are responsible for the transcriptional regulation of Agt in the kidney have not been reported. In the present study, we found that the *Agt* gene promoter contains a putative binding site for c-Myc and proved that the binding of c-Myc/HDAC1 complex to the site is critical for Agt transcription. HFD-induced nuclear accumulation of c-Myc and interaction with HDAC1 were reversed by FK228. Moreover, inhibition of c-Myc by 10058-F4 treatment effectively lowered both systolic and diastolic BP with decrease of renal Agt expression induced by HFD. In addition, c-Myc gene silencing in the HRPTEpi cell also decreased Agt transcription, suggesting that the roles of c-Myc on renal Agt regulation is conserved at least between mouse and human (Supplementary Figure 1C). Our model of the HDAC1/c-Myc axis playing a role in HFD-induced hypertension is also supported by the following lines of evidence. First, HFD fuels prostate cancer progression by amplifying the Myc transcriptional program [11]. Second, c-Myc interacts with HDAC1 at the human immunodeficiency virus type 1 promoter [40]. Third, FK228 suppressed c-Myc exhibiting antitumor activity [16]. Further study is deserved for elucidating mechanisms by which HFD drives HDAC1 binding to c-Myc selectively in kidney.

The correlation between acetylation and stability of c-Myc is controversial. Acetylation negatively regulated c-Myc ubiquitination and proteasomal degradation [41]. c-Myc can be targeted by protein deacetylases such as sirtuin 1, which deacetylates c-Myc resulting in decreased c-Myc protein stability to ultimately suppress tumor growth [42]. However, on the contrary, it was reported that HDAC inhibitor treatment induced the acetylation of c-Myc and decreased its protein levels, leading to anticancer effects [12,16]. We also found that c-Myc deacetylation occurred in parallel with its upregulation in vivo

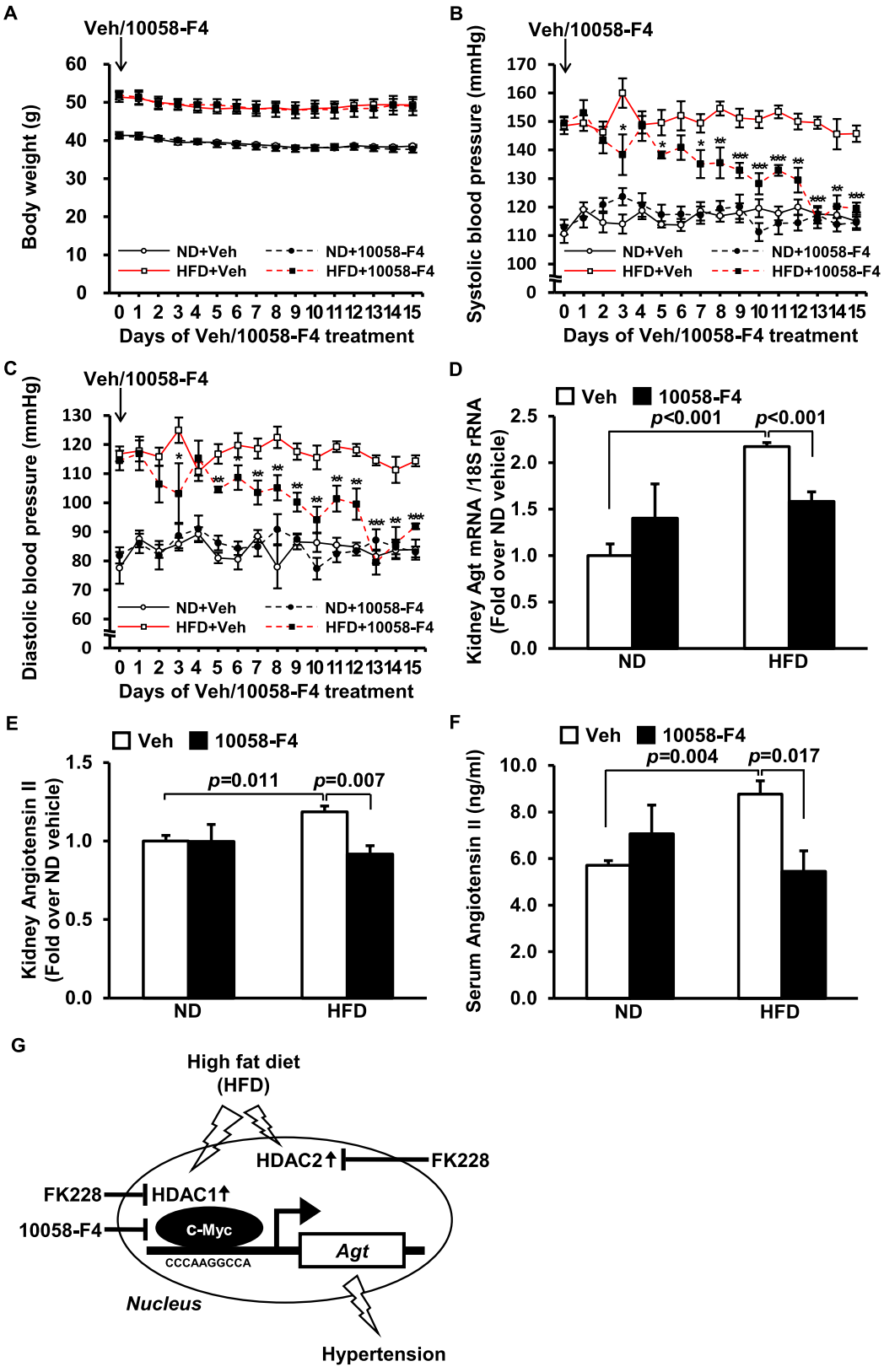

Fig. 7. Effects of c-Myc inhibitor 10058-F4 on HFD-induced renal Agt expression and hypertension. BW (**A**), Systolic BP (**B**), and diastolic BP (**C**) were measured during vehicle or 10058-F4 (20 mg/kg BW per day) administration (* $p < 0.05$, ** $p < 0.01$, and *** $p < 0.001$ HFD+Veh vs. HFD+10058-F4). Graphs summarize the mRNA level of Agt (**D**), and concentration of Ang II in kidney (**E**) and serum (**F**) of ND- or HFD-fed mice after vehicle or 10058-F4 administration. Results are expressed as the mean ± SE (n = 3–6 mice per group). Data were analyzed using the Student's t-test. (**G**) Summary of the results. Veh, vehicle; ND, normal diet; HFD, high-fat diet; Agt, angiotensinogen; BW, body weight; BP, blood pressure; Ang II, angiotensin II; SE, standard error; 18 S rRNA, 18 S ribosomal RNA.

HFD-induced hypertension model, while FK228 treatment decreased c-Myc expression with increased acetylation (Supplementary Figure 2). Interestingly, c-Myc, but not acetylated c-Myc, was found to bind to the c-Myc binding site of *Agt* gene promoter supporting the important role of HDAC1. *In vitro HDAC1* gene silencing also decreased c-Myc expression with increased acetylation (Supplementary Figure 3A, B). HDAC1 and HDAC2 exhibit high homology [43]. In this study, both HDAC1 and HDAC2 were activated by HFD. Unexpectedly, even though silencing of both *HDAC1* and *HDAC2* genes decreased Agt expression (Supplementary Figure 1), HDAC2 did not interact with c-Myc at the *Agt* gene promoter (Fig. 5D, Supplementary Figure 4) nor deacetylate it (Supplementary Figure 3C, D). Thus, in our data, HDAC1 seems to be responsible for deacetylating c-Myc that likely causes degradation. HDAC2 appears to mediate HFD-induced hypertension by a mechanism distinct from that of HDAC1. Further study regarding the role of HDAC2 in HFD-induced hypertension potentially exposes a new group of targets for hypertension treatment.

Our findings reveal that HFD-induced recruitment of deacetylated c-Myc to the *Agt* gene promoter induced by HDAC1 is a critical factor for the renal Agt upregulation and hypertension. We here propose repurposing of the anti-tumor agent FK228 to treat obesity-associated resistant hypertension and highlight c-Myc as a novel therapeutic target for modulating HFD-induced renal Agt expression and hypertension.

Sources of funding

This work was supported by the National Research Foundation of Korea (NRF) grant funded by the Korea government (MSIT) (No. NRF-2020R1A2C2008039).

CRediT authorship contribution statement

Jee In Kim: Conceptualization, Methodology, Software, Validation, Formal analysis, Resources, Writing – original draft, Writing – review & editing, Visualization, Supervision, Project administration, Funding acquisition. **Eui Kyung Youn:** Validation, Formal analysis, Investigation, Data curation, Writing – original draft, Visualization. **Hyun Min Cho:** Validation, Formal analysis, Investigation, Data Curation, Writing – original draft, Visualization. **Jin Ki Jung:** Validation, Formal analysis, Investigation, Data curation, Writing – original draft, Visualization. **Ga-Eun Yoon:** Investigation, Data curation. **Masumi Eto:** Validation, Formal analysis, Writing – review & editing.

Declaration of Competing Interest

None.

Data availability

No data was used for the research described in the article.

Acknowledgments

JIK conceived and designed the research. EKY, HMC, JKJ, and GEY conducted the experiments. JIK, EKY, HMC, JKJ, and ME analyzed and discussed the data. JIK, EKY, HMC, and JKJ prepared the draft. JIK and ME edited the manuscript. We thank Mr. Kwan Beom Lee for the technical support.

Appendix A. Supporting information

Supplementary data associated with this article can be found in the online version at doi:10.1016/j.biopha.2023.114926.

References

[1] I. Kawachi, Physical and psychological consequences of weight gain, J. Clin. Psychiatry 60 (Suppl 21) (1999) 5–9.
[2] A. Oliveras, A. de la Sierra, Resistant hypertension: patient characteristics, risk factors, co-morbidities and outcomes, J. Hum. Hypertens. 28 (4) (2014) 213–217.
[3] W. Kopp, Pathogenesis and etiology of essential hypertension: role of dietary carbohydrate, Med. Hypotheses 64 (4) (2005) 782–787.
[4] C. Soler-Botija, C. Gálvez-Montón, A. Bayés-Genís, Epigenetic biomarkers in cardiovascular diseases, Front Genet 10 (2019) 950.
[5] G.E. Yoon, J.K. Jung, Y.H. Lee, B.C. Jang, J. In Kim, Histone deacetylase inhibitor CG200745 ameliorates high-fat diet-induced hypertension via inhibition of angiotensin II production, Naunyn-Schmiede 'S. Arch. Pharmacol. 393 (3) (2020) 491–500.
[6] J. Choi, S. Park, T.K. Kwon, S.I. Sohn, K.M. Park, J.I. Kim, Role of the histone deacetylase inhibitor valproic acid in high-fat diet-induced hypertension via inhibition of HDAC1/angiotensin II axis, Int J. Obes. (Lond.) 41 (11) (2017) 1702–1709.
[7] J. Díez, A. Panizo, M. Hernández, M.F. Galindo, E. Cenarruzabeitia, F.J. Pardo, Mindán, Quinapril inhibits c-Myc expression and normalizes smooth muscle cell proliferation in spontaneously hypertensive rats, Am. J. Hypertens. 10 (10 Pt 1) (1997) 1147–1152.
[8] J.J. Gildea, H.T. Tran, R.E. Van Sciver, D. Bigler Wang, J.M. Carlson, R.A. Felder, A novel role for c-Myc in G protein-coupled receptor kinase 4 (GRK4) transcriptional regulation in human kidney proximal tubule cells (Dallas, Tex.: 1979), Hypertension 61 (5) (2013), 1021-102.
[9] Z. Ye, X. Lu, Y. Deng, X. Wang, S. Zheng, H. Ren, M. Zhang, T. Chen, P.A. Jose, J. Yang, C. Zeng, In utero exposure to fine particulate matter causes hypertension due to impaired renal dopamine D1 receptor in offspring, Cell Physiol. Biochem 46 (1) (2018) 148–159.
[10] J. Yang, V.A.M. Villar, P.A. Jose, C. Zeng, Renal dopamine receptors and oxidative stress: role in hypertension, Antioxid. Redox Signal 34 (9) (2021) 716–735.
[11] D.P. Labbé, G. Zadra, M. Yang, J.M. Reyes, C.Y. Lin, S. Cacciatore, E.M. Ebot, A. L. Creech, F. Giunchi, M. Fiorentino, H. Elfandy, S. Syamala, E.D. Karoly, M. Alshalalfa, N. Erho, A. Ross, E.M. Schaeffer, E.A. Gibb, M. Takhar, R.B. Den, J. Lehrer, R.J. Karnes, S.J. Freedland, E. Davicioni, D.E. Spratt, L. Ellis, J.D. Jaffe, A.V. D'Amico, P.W. Kantoff, J.E. Bradner, L.A. Mucci, J.E. Chavarro, M. Loda, M. Brown, High-fat diet fuels prostate cancer progression by rewiring the metabolome and amplifying the MYC program, Nat. Commun. 10 (1) (2019) 4358.
[12] A. Nebbioso, V. Carafa, M. Conte, F.P. Tambaro, C. Abbondanza, J. Martens, M. Nees, R. Benedetti, I. Pallavicini, S. Minucci, G. Garcia-Manero, F. Iovino, G. Lania, C. Ingenito, V. Belsito Petrizzi, H.G. Stunnenberg, L. Altucci, c-Myc Modulation and Acetylation Is a Key HDAC Inhibitor Target in Cancer, Clin. Cancer Res.: Off. J. Am. Assoc. Cancer Res. 23 (10) (2017) 2542–2555.
[13] K.M. VanderMolen, W. McCulloch, C.J. Pearce, N.H. Oberlies, Romidepsin (Istodax, NSC 630176, FR901228, FK228, depsipeptide): a natural product recently approved for cutaneous T-cell lymphoma, J. Antibiot. (Tokyo) 64 (8) (2011) 525–531.
[14] Y. Sasakawa, Y. Naoe, T. Inoue, T. Sasakawa, M. Matsuo, T. Manda, S. Mutoh, Effects of FK228, a novel histone deacetylase inhibitor, on human lymphoma U-937 cells in vitro and in vivo, Biochem. Pharmacol. 64 (7) (2002) 1079–1090.
[15] T. Ro, N. Nakayama, H. Achiwa, T. Ohtsu, [Romidepsin (Istodax(R) for intravenous injection 10 mg): pharmacokinetics, pharmacodynamics and clinical study outcome], Nihon yakurigaku zasshi, Folia Pharmacol. Jpn. 151 (3) (2018) 122–129.
[16] Y. Sasakawa, Y. Naoe, T. Inoue, T. Sasakawa, M. Matsuo, T. Manda, S. Mutoh, Effects of FK228, a novel histone deacetylase inhibitor, on tumor growth and expression of p21 and c-myc genes in vivo, Cancer Lett. 195 (2) (2003) 161–168.
[17] J.I. Kim, High fat diet confers vascular hyper-contractility against angiotensin II through upregulation of MLCK and CPI-17, Korean J. Physiol. Pharmacol.: Off. J. Korean Physiol. Soc. Korean Soc. Pharmacol. 21 (1) (2017) 99–106.
[18] Y. Shi, Y. Fu, X. Zhang, G. Zhao, Y. Yao, Y. Guo, G. Ma, S. Bai, H. Li, Romidepsin (FK228) regulates the expression of the immune checkpoint ligand PD-L1 and suppresses cellular immune functions in colon cancer, Cancer Immunol., Immunother.: CII 70 (1) (2021) 61–73.
[19] R. Sakimura, K. Tanaka, F. Nakatani, T. Matsunobu, X. Li, M. Hanada, T. Okada, T. Nakamura, Y. Matsumoto, Y. Iwamoto, Antitumor effects of histone deacetylase inhibitor on Ewing's family tumors, Int. J. Cancer 116 (5) (2005) 784–792.
[20] R. Furumai, A. Matsuyama, N. Kobashi, K.H. Lee, M. Nishiyama, H. Nakajima, A. Tanaka, Y. Komatsu, N. Nishino, M. Yoshida, S. Horinouchi, FK228 (depsipeptide) as a natural prodrug that inhibits class I histone deacetylases, Cancer Res 62 (17) (2002) 4916–4921.
[21] J.P. Montani, V. Antic, Z. Yang, A. Dulloo, Pathways from obesity to hypertension: from the perspective of a vicious triangle, Int J. Obes. Relat. Metab. Disord. 26 Suppl 2 (2002) S28–S38.
[22] A.R. Brasier, J. Li, Mechanisms for inducible control of angiotensinogen gene transcription (Dallas, Tex.: 1979), Hypertension 27 (3 Pt 2) (1996) 465–475.
[23] H.S. Kim, J.H. Krege, K.D. Kluckman, J.R. Hagaman, J.B. Hodgin, C.F. Best, J. C. Jennette, T.M. Coffman, N. Maeda, O. Smithies, Genetic control of blood pressure and the angiotensinogen locus, Proc. Natl. Acad. Sci. USA 92 (7) (1995) 2735–2739.
[24] T. Matsusaka, F. Niimura, A. Shimizu, I. Pastan, A. Saito, H. Kobori, A. Nishiyama, I. Ichikawa, Liver angiotensinogen is the primary source of renal angiotensin II, J. Am. Soc. Nephrol. 23 (7) (2012) 1181–1189.
[25] L.G. Navar, A. Nishiyama, Why are angiotensin concentrations so high in the kidney? Curr. Opin. Nephrol. Hypertens. 13 (1) (2004) 107–115.

[26] H. Kobori, Y. Ozawa, Y. Suzaki, M.C. Prieto-Carrasquero, A. Nishiyama, T. Shoji, E. P. Cohen, L.G. Navar, Young Scholars Award Lecture: Intratubular angiotensinogen in hypertension and kidney diseases, Am. J. Hypertens. 19 (5) (2006) 541–550.
[27] A. Nishiyama, H. Kobori, Independent regulation of renin-angiotensin-aldosterone system in the kidney, Clin. Exp. Nephrol. 22 (6) (2018) 1231–1239.
[28] H. Kobori, A. Nishiyama, L.M. Harrison-Bernard, L.G. Navar, Urinary angiotensinogen as an indicator of intrarenal Angiotensin status in hypertension, Hypertension 41 (1) (2003) 42–49.
[29] H. Kobori, L.M. Harrison-Bernard, L.G. Navar, Urinary excretion of angiotensinogen reflects intrarenal angiotensinogen production, Kidney Int 61 (2) (2002) 579–585.
[30] P. Rivera, C. Miranda, N. Roldán, A. Guerrero, J. Olave, P. Cárdenas, Q.M. Nguyen, M. Kassan, A.A. Gonzalez, Augmented transcripts of kidney injury markers and renin angiotensin system in urine samples of overweight young adults, Sci. Rep. 10 (1) (2020) 21154.
[31] V. Reverte, V.R. Gogulamudi, C.B. Rosales, D.C. Musial, S.R. Gonsalez, A.J. Parra-Vitela, M. Galeas-Pena, V.N. Sure, B. Visniauskas, S.H. Lindsey, P.V.G. Katakam, M. C. Prieto, Urinary angiotensinogen increases in the absence of overt renal injury in high fat diet-induced type 2 diabetic mice, J. Diabetes Complicat. 34 (2) (2020), 107448.
[32] M. Kukida, L. Cai, D. Ye, H. Sawada, Y. Katsumata, M.K. Franklin, P.I. Hecker, K. S. Campbell, A.H.J. Danser, A.E. Mullick, A. Daugherty, R.E. Temel, H.S. Lu, Renal angiotensinogen is predominantly liver derived in nonhuman primates, Arterioscler. Thromb. Vasc. Biol. 41 (11) (2021) 2851–2853.
[33] D.M. Bovée, L. Ren, E. Uijl, M.C. Clahsen-van Groningen, R. van Veghel, I. M. Garrelds, O. Domenig, M. Poglitsch, I. Zlatev, J.B. Kim, S. Huang, L. Melton, X. Lu, E.J. Hoorn, D. Foster, A.H.J. Danser, Renoprotective effects of small interfering RNA targeting liver angiotensinogen in experimental chronic kidney disease, Hypertension 77 (5) (2021) 1600–1612.
[34] E.S. Morgan, Y. Tami, K. Hu, M. Brambatti, A.E. Mullick, R.S. Geary, G.L. Bakris, S. Tsimikas, Antisense Inhibition of Angiotensinogen With IONIS-AGT-L(Rx): Results of Phase 1 and Phase 2 Studies, JACC Basic Transl. Sci. 6 (6) (2021) 485–496.
[35] N. Ramkumar, D. Stuart, J. Ying, D.E. Kohan, A possible interaction between systemic and renal angiotensinogen in the control of blood pressure, Am. J. Hypertens. 26 (4) (2013) 473–480.
[36] M. Koizumi, K. Ueda, F. Niimura, A. Nishiyama, M. Yanagita, A. Saito, I. Pastan, T. Fujita, M. Fukagawa, T. Matsusaka, Podocyte injury augments intrarenal angiotensin II generation and sodium retention in a megalin-dependent manner, Hypertension 74 (3) (2019) 509–517.
[37] H. Lin, F. Geurts, L. Hassler, D. Batlle, K.M. Mirabito Colafella, K.M. Denton, J. L. Zhuo, X.C. Li, N. Ramkumar, M. Koizumi, T. Matsusaka, A. Nishiyama, M. J. Hoogduijn, E.J. Hoorn, A.H.J. Danser, Kidney angiotensin in cardiovascular disease: formation and drug targeting, Pharm. Rev. 74 (3) (2022) 462–505.
[38] F. Yang, N. Zhao, D. Ge, Y. Chen, Next-generation of selective histone deacetylase inhibitors, RSC Adv. 9 (34) (2019) 19571–19583.
[39] A. Rana, S. Jain, N. Puri, M. Kaw, N. Sirianni, D. Eren, B.R. Mopidevi, A. Kumar, The transcriptional regulation of the human angiotensinogen gene after high-fat diet is haplotype-dependent: Novel insights into the gene-regulatory networks and implications for human hypertension, PloS One 12 (5) (2017), e0176373.
[40] G. Jiang, A. Espeseth, D.J. Hazuda, D.M. Margolis, c-Myc and Sp1 contribute to proviral latency by recruiting histone deacetylase 1 to the human immunodeficiency virus type 1 promoter, J. Virol. 81 (20) (2007) 10914–10923.
[41] A.S. Farrell, R.C. Sears, MYC degradation, Cold Spring Harb. Perspect. Med 4 (3) (2014).
[42] J. Yuan, K. Minter-Dykhouse, Z. Lou, A. c-Myc-SIRT1, feedback loop regulates cell growth and transformation, J. Cell Biol. 185 (2) (2009) 203–211.
[43] I.V. Gregoretti, Y.M. Lee, H.V. Goodson, Molecular evolution of the histone deacetylase family: functional implications of phylogenetic analysis, J. Mol. Biol. 338 (1) (2004) 17–31.